The flow field for the thicker guide vane is shown in Fig.12(c) and we find the flow stagnation disappears. The design method of the return guide vane which covers the region of the flow separation is effective for the suppression of the stagnation, although the method is a trial-and-error method. In the case with the small number of the vanes such as 5, the vane is quite thick and the flow stagnation can occur near the trailing edge of the vane. Then, we designed the guide vane which covered the region of the flow separation shown in Fig.12(a) for 9 vanes. The flow field for 9 thick guide vanes is shown in Fig.12(d). Although the result is for another pump similar to the present pump, the flow separation is suppressed and the circumferential velocity is decreased well. It was found that the design method of the return guide vane which covers the region of the flow separation is effective for the suppression of the stagnation. We also found that the increase of the number of the vanes leads to the decrease of the region of the flow separation and the vane thickness and is effective for decreasing the circumferential velocity well at the outlet of the return channel.

The amplitude of the pressure fluctuation at the outlet was from -13% to +10% of the average values in the original pump and was from -7% to +4% in the pump with five thicker vanes. In both cases, the pressure fluctuations were mainly caused by the interaction of the wake of the impeller and the tongue of the double volute casing because of the smaller clearance of 2 mm between the outlet of the impeller and the tongue of the double volute casing, although the geometry of the return guide vanes affect the pressure fluctuation at the outlet to a certain degree. As the pump with 9 thicker vanes has the larger clearance of 7 mm between the outlet of the impeller and the tongue of the double volute casing, the amplitude of the pressure fluctuation at the outlet was smaller and about ±1% of the average values. Therefore, as you know, the larger clearance between the outlet of the impeller and the tongue of the volute casing is effective for the suppression of the pressure fluctuation. The larger distance is also effective for the decrease of the shear stress on the tongue, which is reported in detail in the next paper.

6. Conclusions

We carried out the research on the development of a two-stage centrifugal blood pump for the cardiopulmonary support system. The two-stage blood pump in the present study is characterized by higher discharge pressure at low peripheral speed of the impeller. The results obtained in the present study are summarized as follows.

(1) The slope of the performance curve of the prototype is larger. This means that the prototype has useful characteristics that the flow rate is insensitive to the resistance.
(2) The higher shear stress which can cause the hemolysis occurs on the casing near the tip of the impeller and the flow stagnation which can be a cause of the thrombosis occurs in the return channel if we design a centrifugal blood pump with a low type number and a semi-open impeller, mainly based on the design method for general industrial pumps.
(3) The enlargement of the tip clearance was not effective for decreasing the wall shear stress on the casing near the tip of the impeller.
(4) The front shroud of the impeller suppresses the interaction between the secondary flow and the casing and can decrease the wall shear stress on the casing near the tip of the impeller. As the front shroud increases the pump head, it can be useful to increase the anti-hemolysis performance by decreasing the rotational speed of the impeller.
(5) It was found that the design method of the return guide vane which covers the region of the flow separation is effective for the suppression of the stagnation. We also found that the increase of the number of the vanes leads to the decrease of the region of the flow separation and the vane thickness and is effective for decreasing the circumferential velocity well at the outlet of the return channel.

Improvements of the present pump and the result of the hemolysis test are reported in a next paper.

Acknowledgments

The present study was supported by JSPS Grant-in-Aid for Scientific Research (B) (Grant Number 18360094, Principal Investigator: Dr. Tomonori Tsukiya).

Nomenclature

C	Tip clearance	ν	Kinetic viscosity
D_t	Diameter of impeller	θ	Circumferential coordinate
h	Blade height	ρ	Fluid density
N	Rotational speed	τ	Shear stress
Q	Volumetric flow rate	**Subscript**	
Re	Reynolds number ($=U_tD_t/\nu$)	1	Inlet
u	Flow velocity	2	Outlet
U_t	Tip speed of impeller	*blood*	Blood
β	Blade angle	d	Reference
Δp	Pressure difference	*water*	Water
μ	Viscosity	θ	Circumferential component

References

[1] Horiguchi, H., Tsukiya, T., Takemika, T., Nomoto, T., and Tsujimoto, Y., 2013, "Improvement of Two-Stage Centrifugal Blood Pump for Cardiopulmonary Support System and Evaluation of Anti-Hemolysis Performance (in Japanese)," Transactions of the

JSME, Series B, Vol. 79, No. 800, pp. 11-23.
[2] Lou, S., MacLaren, G., Best D., Delzoppo, C., and Butt, W., 2014, "Hemolysis in Pediatric Patients Receiving Centrifugal-Pump Extracorporeal Membrane Oxygenation: Prevalence, Risk Factors, and Outcomes," Critical Care Medicine, Vol. 42, No. 5, pp. 1213-1220.
[3] Takeda, H., 2005, "Basic Design on Pumps (in Japanese)," Dengyosha Technical Review, Vol. 29, No. 2, pp. 7-14. (http://www.dmw.co.jp/technical/pdf/no57.pdf)
[4] Schima, H., Muller, M. R., Papantonis, D., Schlusche, C., Huber, L., Schmidt, C., Trubel, W., Thoma, H., Losert, U., and Wolner, E., 1993, "Minimization of Hemolysis in Centrifugal Blood Pumps: Influence of Different Geometries," The International Journal of Artificial Organs, Vol. 16, No. 7, pp. 521-529.
[5] Miyazoe, Y., Sawairi, T., Ito, K., Konishi, Y., Yamane, T., Nishida, M, Masuzawa, T., Takiura, K., and Taenaka, Y., 1998, "Computational Fluid Dynamic Analysis to Establish Design Process of Centrifugal Blood Pumps," Artificial Organs, Vol. 22, No. 5, pp. 381-385.
[6] Masuzawa, T., Tsukiya, T., Endo, S., Tatsumi, E., Taenaka, Y., Yamane, T., Nishida, M., Asztalos, B., Miyazoe, Y., Ito, K., Sawairi, T., and Konishi, Y., 1998, "Effect of Gaps Between Impeller Tip and Casing Wall upon Hemolysis Property of a Centrifugal Blood Pump (in Japanese)," Journal of Life Support Engineering, Vol. 10, No. 3, pp. 102-105. (https://www.jstage.jst.go.jp/article/lifesupport1996/10/3/10_3_102/_pdf)
[7] ANSYS, Inc., 2006, "Modeling Flow Near the Wall", ANSYS CFX-Solver Modeling Guide, Release 11, pp.125-127.
[8] ANSYS, Inc., 2006, "Modeling Flow Near the Wall", ANSYS CFX-Solver Theory Guide, Release 11, pp.110-111.
[9] Kameneva, M. V., Burgreen, G. W., Kono, K., Repko, B., Antaki, J. F., and Umezu, M., 2004, "Effects of Turbulent Stresses upon Mechanical Hemolysis: Experimental and Computational Analysis," ASAIO Journal, Vol. 50, No. 5, pp. 418-423.
[10] Kurokawa, J., Choi, Y-D., Ishii, M., Matsui, J., and Imamura, H., 2003, "Theoretical Head of Semi-Open Impeller," Proceedings of the 7th Asian International Conference on Fluid Machinery, No. 40030, pp. 1-7.

J Artif Organs
DOI 10.1007/s10047-014-0811-z

ORIGINAL ARTICLE

Artificial Heart (Basic)

Development of a flow rate monitoring method for the wearable ventricular assist device driver

Kentaro Ohnuma · Akihiko Homma · Hirohito Sumikura · Tomonori Tsukiya · Yoshiaki Takewa · Toshihide Mizuno · Hiroshi Mukaibayashi · Koichi Kojima · Kazuo Katano · Yoshiyuki Taenaka · Eisuke Tatsumi

Received: 9 July 2014 / Accepted: 5 December 2014

Abstract Our research institute has been working on the development of a compact wearable drive unit for an extracorporeal ventricular assist device (VAD) with a pneumatically driven pump. A method for checking the pump blood flow on the side of the drive unit without modifying the existing blood pump and impairing the portability of it will be useful. In this study, to calculate the pump flow rate indirectly from measuring the flow rate of the driving air of the VAD air chamber, we conducted experiments using a mock circuit to investigate the correlation between the air flow rate and the pump flow rate as well as its accuracy and error factors. The pump flow rate was measured using an ultrasonic flow meter at the inflow and outflow tube, and the air flow was measured using a thermal mass flow meter at the driveline. Similarity in the instantaneous waveform was confirmed between the air flow rate in the driveline and the pump flow rate. Some limitations of this technique were indicated by consideration of the error factors. A significant correlation was found between the average pump flow rate in the ejecting direction and the average air flow rate in the ejecting direction (R^2 = 0.704–0.856), and the air flow rate in the filling direction (R^2 = 0.947–0.971). It was demonstrated that the average pump flow rate was estimated exactly in a wide range of drive conditions using the air flow of the filling phase.

Keywords Flow rate monitoring · Wearable pneumatic drive unit · Ventricular assist devices (VADs) · Air mass flow

K. Ohnuma (✉) · H. Sumikura · T. Tsukiya · Y. Takewa · T. Mizuno · Y. Taenaka · E. Tatsumi
Department of Artificial Organs, National Cerebral and Cardiovascular Center Research Institute, 5-7-1 Fujishirodai, Suita-shi, Osaka 565-8565, Japan
e-mail: ohnuma.kentaro@ri.ncvc.go.jp

A. Homma · K. Katano
School of Science and Engineering, Tokyo Denki University, Saitama, Japan

H. Mukaibayashi · K. Kojima
IWAKI Co., Ltd., Saitama, Japan

Introduction

Mechanical circulatory support using ventricular assist devices (VADs) has become a major option in the treatment of severe heart failure. Early VADs were used mainly as a bridge to heart transplantation (BTT). For BTT patients to be discharged and stay at home, the blood pump needs to be implanted; therefore, a wide variety of implantable devices have been developed [1, 2]. Annually, more than 1,000 patients are implanted with the current devices that use compact rotary pumps [2–4]. An overwhelming shortage of donor organs, however, is still a serious problem globally. Organ transplantation from brain-death donors was approved in 1997 in Japan [5], but the accumulative number of heart transplantations as of December 2013 was only 186.

Before two types of implantable VADs were approved in Japan in 2010 [6], the extracorporeal VAD with a pneumatically driven pump, originally developed at the National Cerebral and Cardiovascular Center, was the only VAD available in Japan (currently available as Nipro VAD, Nipro, Osaka, Japan) [7–11]. More than 900 patients have been treated with Nipro VAD, and about 50 patients are almost always being treated with this system in Japan [12]. The Nipro VAD has played an important role as a chronic-use device for patients, who are outside the

Published online: 13 December 2014

application range of transplantation or not suitable for implantable VAD due to small body size, or as a temporary support for a bridge to decision [2, 6] in the acute severe heart failure patients.

The conventional driver of this pneumatic VAD is equipped with an air compressor, vacuum pump, and batteries. These components, however, make the driver heavy and bulky, which restricts the activity of the patients. Downsizing of the pneumatic VAD driver is one of the key factors for improving the patient's QOL by expanding the range of actions. The authors developed a portable driver for the Nipro VAD, the Mobart-NCVC driver (Senko Medical Instrument Manufacturing Co., Ltd.), which allows transportation in the hospital by the patient himself, and also enables long-distance transportation of patients from one institute to another for heart transplantation. The Mobart-NCVC uses an electro-hydraulic actuator and weighs 13 kg [13].

Our research institute has been working on the development of a more compact VAD driver consisting of a cylinder-piston actuator [14]. The current model of this driver, including its two batteries, weighs only 4.7 kg. The pump can be operated with the two batteries for more than 5 h under normal operating conditions. We are planning to add an additional flow meter to this driver, which will be useful to optimize the operating conditions of the VAD. A mass flow meter, which is capable of measuring the instantaneous flow rates of the driving air in the VAD air chamber, has been employed to calculate blood flow through the VAD. The present study introduces the air flow meter for our portable VAD driver and examines accuracy and errors of it in relation to the pump flow through experiments using a mock circuit. Correction methods for obtaining blood flow rates from the air flow rates are also investigated.

Materials and methods

Description of Nipro VAD blood pump

The Nipro VAD blood pump is a pneumatically driven diaphragm pump, as shown in Fig. 1b. The blood pump is mainly made from polyurethane resin (TM3) and consists of two mechanical heart valves. The priming volume of the blood pump is 70 mL, and is capable of generating 50–60 mL of blood flow per beat.

Wearable pneumatic drive unit (WPD)

The structure of the mechanism in the WPD for generating air pressure is depicted in Fig. 1. Air pressure to drive the diaphragm of the blood pump is generated by converting the rotation of the brushless DC motor into linear motion via a crankshaft directly connected to the cylinder piston. The internal capacity of this cylinder piston is 109 mL. Two regulating valves at the air outlets adjust the driving positive or negative pressure by releasing or drawing the air from or into the tube. The ratio of systole duration (SD) is predetermined by the built-in noncircular gears [14]. The current model of the WPD is also equipped with a pressure release valve at the bottom dead center to compensate for any change in the amount of air in the air circuit due to air leaks from pressure control or changes in room air conditions. The top dead center and bottom dead center of the cylinder piston can be detected with built-in proximity sensors. The experiments in the present study were conducted using three drive units with SD ratios of 35, 40, and 45 % (WPD100-SD35, SD40, and SD45).

Measurement of air flow rates

Figure 2 shows the experimental setup. The Nipro VAD blood pump was connected to an overflow-type mock circuit (IWAKI Co., Ltd.). The working fluid was tap water at 25 °C. The WPD was connected to the Nipro VAD via a 1.35-m air driveline. The air flow rates in the driveline were measured using a thermal gas mass flow meter (model 4043, TSI Inc.), which was installed in the driveline 750 mm away from the blood pump. This mass flow meter possesses a good accuracy (up to 2 % or 0.05 L/min) and response (4 ms) with low resistance. The measurement of the reverse flow with this flow meter has the uncertainty of 2.5 % of the reading in comparison with it of the flow of the forward direction. The forward direction of the flow meter was set as the ejecting direction of VAD. The flow rates of the blood pump were measured using ultrasonic flow meters (T106, Transonic Systems Inc.) installed in the tubes on the inflow and outflow sides of the pump. The air pressures of the WPD were measured using piezoelastic pressure transducers (PA-500, Nidec Copal Electronics Corp.). The position of the cylinder piston was detected from the pulse signals at the top dead center and bottom dead center of the cylinder piston. The flow meter was able to output the volumetric flow rates under a standard condition (at 21.11 °C and 101.3 kPa). Because the pressure in the driveline widely varied during pump operation, flow rates were corrected using the following equation:

$$Q_{\mathrm{aVF}} = Q_{\mathrm{aStdF}}\left[\frac{273.15+T}{273.15+21.11}\right]\left[\frac{759.8}{759.8+P}\right] \quad (1)$$

where $Q_{\mathrm{a\ VF}}$ is the converted volumetric flow rate of the air driveline, $Q_{\mathrm{a\ StdF}}$ is the reading from the flow meter, P is the pressure of the driveline, and T is temperature of the air (°C). T was approximately assumed room temperature because it was difficult to exactly measure the

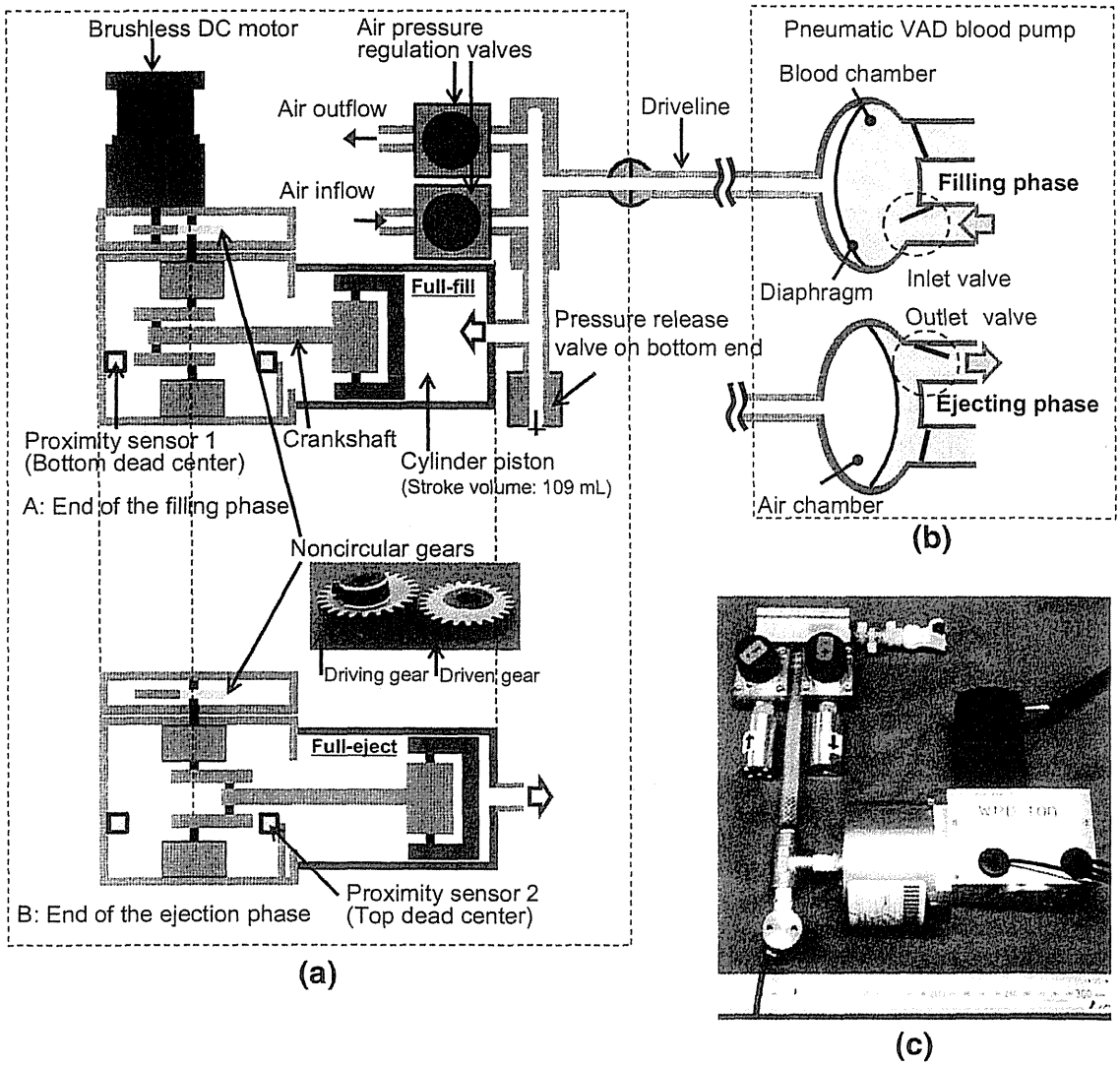

Fig. 1 Overview of the WPD-100 drive unit. **a** WPD-100 mechanism for generating air pressure. **b** Mechanism for generating pulsatile flow on the pneumatic blood pump. **c** Photograph of the core unit, air regulation valves and pressure release valves

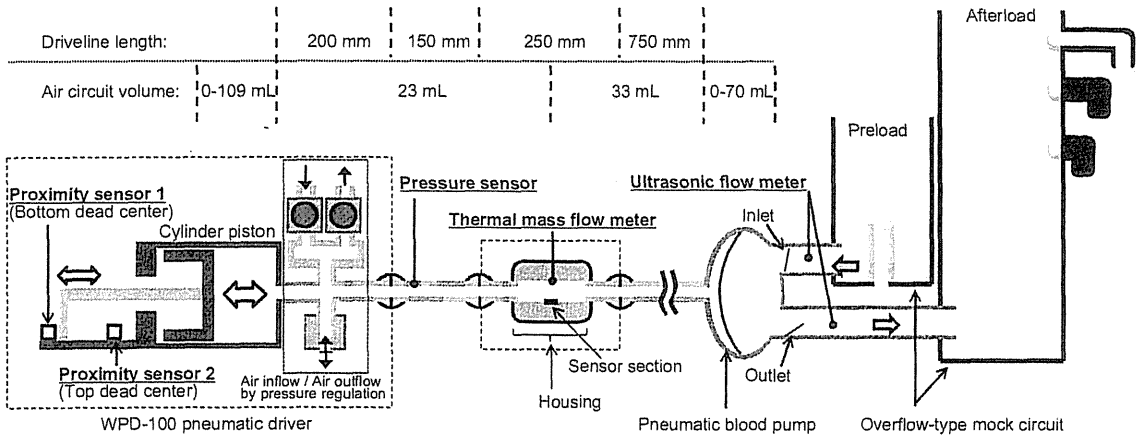

Fig. 2 Schematic diagram of equipment composition and the experimental circuit (air circuit of the pneumatic driver side and mock circuit of the pump output side)

instantaneous value of air temperature in the driveline with high responsiveness.

Test conditions

The preload to the blood pump was kept constant at 10 mmHg using the overflow-type mock circuit, and the afterload was set to 80, 100, and 120 mmHg, respectively. The measurements were conducted with SD ratios of 35, 40, and 45 % using the three types of drive units, and beating rates of 60, 70, 80, 90, and 100 bpm. The pressure of the blood pump was adjusted using the air pressure regulation valves of the drive unit so that almost full filling and full ejection driving was achieved by visual inspection.

Results

Figure 3 shows an example waveform when the blood pump was driven by WPD100-SD40 at 70 bpm, with an afterload of 100 mmHg and a preload of 10 mmHg. The output from the air flow meter demonstrated sufficient response to the ejection and the filling of the VAD. The output of the air flow meter, $Q_{a\ StdF}$, during the filling phase was positive in Fig. 3b because all the air flow passed through the sensor is output as a signal of positive direction, and does not indicate the direction of the air flow. Based on the signal of the proximity sensors of the WPD, we were able to easily divide the waveform into the ejecting phase and the filling phase and to change the waveform direction of the filling phase into the real flow direction as shown in Fig. 3d.

Reflux components generated by the mechanical valve that are not reflected in the air flow rate and flow components for a period during which the inflow and outflow of the pump occur simultaneously were detected (Fig. 3c). Similar trends were also obtained under other driving conditions (Fig. 4a, b). The average of the reflux components shown in Fig. 4a was 0.69 ± 0.077 L/min. Ratios of the flow component shown in Fig. 4b to the pump flow rate were a maximum of 3.9 % (SD 35 %, HR: 100 bpm, afterload: 80 mmHg) and a minimum of 1.3 % (SD 45 %, HR: 60 bpm, afterload: 120 mmHg) under all test conditions.

Figure 3d shows a comparison between the converted air flow rates, $Q_{a\ VF}$, and the blood flow rates, Q_p. During ejection, phase deviation between the air and blood was observed due to compressibility. The deviation is illustrated as the shadowed area between the waveforms of the air flow rate and the blood flow rate in Fig. 3d. The Nipro VAD employs active filling via the negative pressure generated by the vacuum pump in the console, but the deviation was found to be smaller during the filling phase. Similar trends were also obtained under other driving conditions. Except for this deviation, there is sufficient similarity of the outputs from the air flow meter to those from the blood flow meter.

As one example, the significant deviations during the ejecting phase at SD40 are shown in Fig. 4c as the capacity in one cycle under each driving condition. The capacity of the air circuit in the latter part of the air flow meter was approximately 103 mL at the end of the pump ejection phase and approximately 33 mL at the end of the filling phase. As shown in Fig. 4c, the capacity required for compression to raise the pressure of the air of this capacity from 0 to 250 mmHg (approximate value of the maximum driving pressure) was calculated as 18.9 mL from the capacity of the air circuit at the end of the ejection phase and as 6.1 mL from the capacity at the end to the filling phase, using formulae of changes in gas state (2) and (3), where polytropic index, n was set to 1.4.

$$PV^n = \text{const.} \tag{2}$$

$$\frac{V_1}{V_2} = \left(\frac{P_2}{P_1}\right)^{\frac{1}{n}} \tag{3}$$

The average flow rates were obtained by integrating the flow rate waveforms obtained for the ejecting and filling periods. The correlations of the pump outlet flow rate during the ejecting phase and the air flow rates during the ejecting phase are shown in Fig. 5a, and the pump outlet flow rate during the ejecting phase and the air flow rates during the filling phase are shown in Fig. 5b. Good linearity was found in the average air flow rates in the filling directions (in the forward direction, SD45: $R^2 = 0.781$, SD40: $R^2 = 0.704$, SD35: $R^2 = 0.856$; and in the backward direction, SD45: $R^2 = 0.969$, SD40: $R^2 = 0.947$, SD35: $R^2 = 0.971$). However, deviations from the blood flow meter were found both in the ejecting and filling directions. The average flow rate measured by the air flow meter was approximately 90 % lower than that measured by the blood flow meter in the forward direction and approximately 120 % higher in the backward direction.

Discussion

In this study, similarity in the instantaneous waveform was confirmed between the air flow rate in the driveline and the pump flow rate. A significant correlation was particularly recognized between the average blood flow rates and the air flow rates of the filling direction. On the other hand, some limitations of this technique were suggested by the deviation between the air flow and blood flow observed due to compressibility of the air and the error factors that were not reflected in the air flow, as described below.

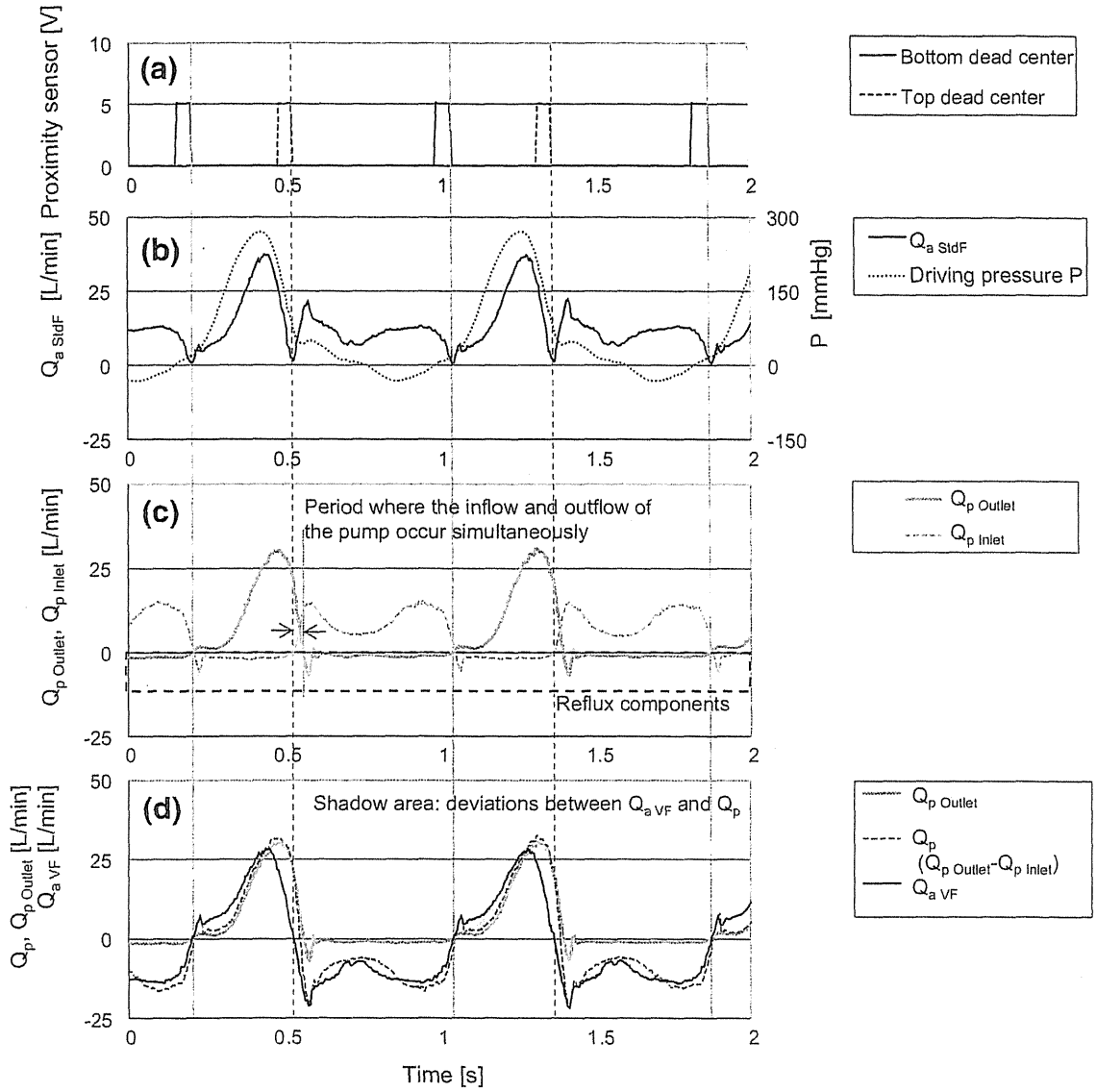

Fig. 3 Example of instantaneous waveforms when the blood pump was driven by WPD100-SD40 at 70 bpm, with an afterload of 100 mmHg. **a** Positions of the cylinder piston detected with proximity sensors, **b** measured air flow and driving pressure, **c** pump flow rate measured at the inlet and outlet sides of the pump, **d** converted volumetric flow rate of the air driveline, $Q_{a\ VF}$, and the flow rates into and out of the blood chamber of the pump, Q_p

Error factors that were not reflected in the air flow

Deviations between the air flow and blood flow could be attributed to several causes. For instance, there may be components that flow due to inertia during the period where the inflow and outflow of the pump occur simultaneously, as shown in Figs. 3c and 4b. This phenomenon is remarkable, especially at higher beating rates. The effect of this flow is not reflected in the air flow because it does not cause any volumetric changes in the blood pump chamber. However, any flow rate not generated by movement of the diaphragm has the range from 1.3 to 3.9 % under any test condition, so it was considered that these flow rates negligibly influence the estimation of flow rate. Similarly, reflux components generated by the mechanical valve are not reflected in the air flow rate (Figs. 3c, 4a). However, it was considered from Fig. 4a that the reflux components could be corrected using a constant term in the estimate of the pump flow rate.

The point that the room temperature was used when converting the volumetric air flow rate can be cited as another error factor. The air temperature in the driveline measured with the temperature sensor to be built into the air flow meter was up to 38 °C under all test conditions (response time of the sensor: 75 ms, room temperature: 25 °C). Compared with the volumetric air flow converted

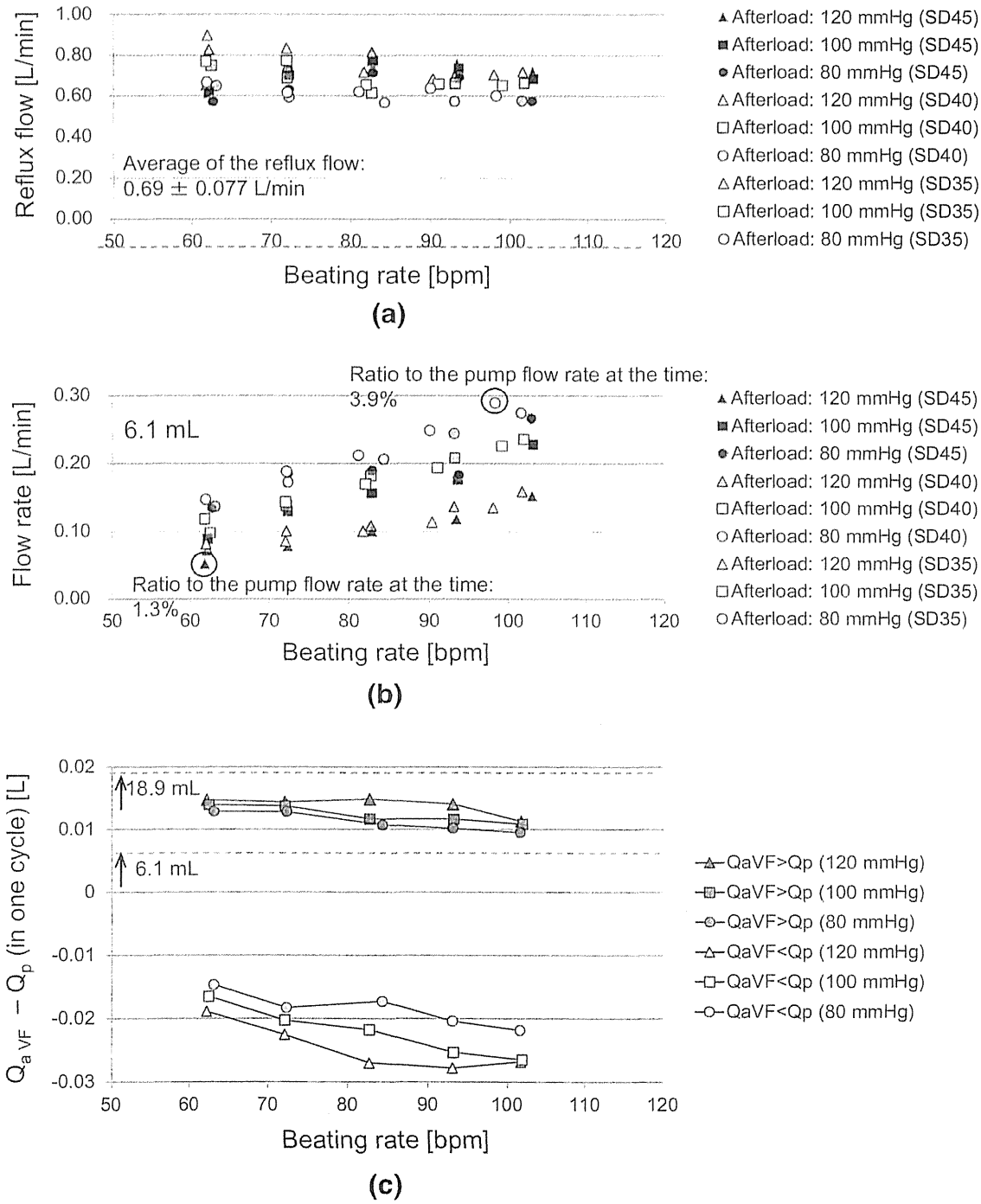

Fig. 4 Deviations between the air flow and blood flow. **a** Reflux components generated by the mechanical. **b** Flow components for a period during which the inflow and outflow of the pump occur simultaneously. **c** Example of differences between $Q_{a\ VF}$ and Q_p during one cycle with WPD-100 SD40

with room temperature, the air flow converted with the air temperature in the driveline is increased up to 4.3 % from Eq. (1). The influence of the temperature is considered to be limited, the use of a higher responsive temperature sensor, however, will be able to contribute to improve the accuracy of the measurement of the volumetric air flow.

Deviation due to compressibility of the air

As shown in Fig. 3d, the deviation between the air flow rates and blood flow rates is apparently larger during the ejecting phase than during the filling phase. From the results shown in Figs. 3d and 4c, the capacity difference in

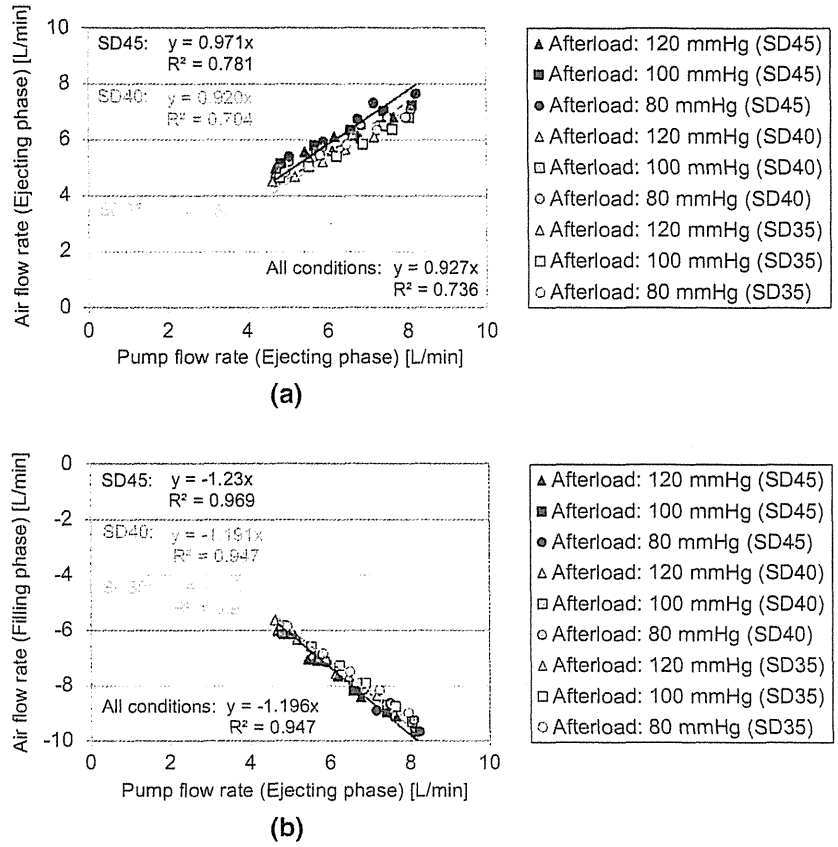

Fig. 5 Correlation between the average pump flow rate in the ejecting direction and the average air flow rate. **a** The air flow rates during the ejecting phase. **b** The air flow rates during the filling phase

the initial stage of ejection was found to be within the range of 6.1–18.9 mL. The deviation in the initial stage of ejection was considered to be mainly caused by the compression process of the air.

During the latter half of the ejection phase, the fluid flow on the blood chamber side of the pump generated by volumetric expansion of the air while releasing the driving pressure in the air chamber of the pump to push out the diaphragm after passing through the sensor section of the air flow meter (an element that is hardly reflected in the air flow meter) was considered to be the main factor causing the deviation.

During the filling phase, on the other hand, the magnitude of the negative pressure is relatively low, and the difference in the flow rate was smaller than that during the ejection phase.

Linearity of the average flow rate

As shown in Fig. 5a, b, the linearity of the average flow rate was higher in the air flow rate of the filling direction than that of the ejecting direction, because of the deviation with compressibility of the air during the ejecting phase and the volumetric air flow conversion with room temperature. The deviations from the blood flow meter were slightly low for the air flow rate of the ejecting direction. The estimation error of the average blood flow likely decreases under a wide range of driving conditions because of the high linearity when the air flow rate in the filling direction is used. Furthermore, estimation of the pump flow rate is considered stable and fully possible using our method because of high correlation with the pump flow and the air flow.

Practical application and availability

In the present study, the conversion from the standard air flow rate to the volumetric flow rate and the calculation of the average flow rate were performed offline. For practical applications, the estimate of the pump flow rate should be automatically calculated in real time, using the air flow of the filling direction. This is feasible using a general microprocessor because of the simple algorithm using the proximity sensors of the WPD and the linearity between the pump flow rate and the air flow rate. The air flow meter was installed in the driveline in this experiment. The flow meter should be installed into the WPD system not to impair the portability of the WPD. This problem was considered to be solved using a small embedded flow sensor.

It is possible, of course, to measure the blood flow rate in a pneumatic VAD using an ultrasonic flow meter, but the

flow meter needs to be built into the system for a patient to be able to carry it around. It is necessary for the probe to be attached to the outflow tube crossing the skin. To date, various, indirect methods for measuring the blood flow rate in a pneumatic blood pump (or the internal capacity of the pump) have been attempted. While techniques that use electric impedance, capacitance, or ultrasonic waves [15–18] are useful for measuring the pump capacity in real time, these techniques require sensors or electrodes to be attached at positions near the blood chamber of the pump housing. Our method of measuring pump blood flow at the side of the drive unit from the air flow without modifying the existing blood pump may have disadvantage for the accuracy and the measurement of the instantaneous value because of estimating the pump flow rate indirectly. It, however, has an advantage of not disturbing the care of sites that the inflow and outflow conduits cross the skin. In addition, it has a sufficient measurement performance of the average pump flow rate.

Conclusion

A flow measurement method for the portable driver of a pneumatically driven VAD using an air flow meter for estimating the pump flow has been investigated. Limitations of this technique were indicated by the deviation between the air flow and blood flow resulting from compressibility of the air and the blood flow components that were not reflected in the air flow. A significant correlation was particularly recognized between the average blood flow rates and the air flow rates of the filling direction. It was demonstrated that the average pump flow rate was estimated exactly in a wide range of drive conditions using the air flow of the filling phase. This technique is useful for monitoring the pump blood flow in the case when a pneumatic VAD is driven by a WPD.

Acknowledgments This study was supported in part by Grant-in-Aid for Scientific Research (B) (No. 24390308) and Grant-in-Aid for Challenging Exploratory Research (No. 25670563) from the Japan Society for the Promotion of Science and the Ministry of Education, Culture, Sports, Science and Technology of Japan.

Conflict of interest The authors declare that they have no conflict of interest.

References

1. Stewart GC, Givertz MM. Mechanical circulatory support for advanced heart failure: patients and technology in evolution. Circulation. 2012;125(10):1304–15.
2. Slaughter MS, Pagani FD, Rogers JG, Miller LW, Sun B, Russell SD, Starling RC, Chen L, Boyle AJ, Chillcott S, Adamson RM, Blood MS, Camacho MT, Idrissi KA, Petty M, Sobieski M, Wright S, Myers TJ, Farrar DJ. Clinical management of continuous-flow left ventricular assist devices in advanced heart failure. J Heart Lung Transplant. 2010;29(45):S1–39.
3. Kirklin JK, Naftel DC, Kormos RL, Stevenson LW, Pagani FD, Miller MA, Baldwin JT, Young JB. The fourth INTERMACS annual report: 4,000 implants and counting. J Heart Lung Transplant. 2012;31(2):117–26.
4. Kirklin JK, Naftel DC, Kormos RL, Stevenson LW, Pagani FD, Miller MA, Baldwin JT, Young JB. Fifth INTERMACS annual report: risk factor analysis from more than 6,000 mechanical circulatory support patients. J Heart Lung Transplant. 2013;32(2):141–56.
5. Ishii M, Hamamoto M. Bioethics and organ transplantation in Japan. JMAJ. 2009;52(5):289–92.
6. Kyo S, Minami T, Nishimura T, Gojo S, Ono M. New era for therapeutic strategy for heart failure: destination therapy by left ventricular assist device. J Cardiol. 2012;59(2):101–9.
7. Shiga T, Kinugawa K, Hatano M, Yao A, Nishimura T, Endo M, Kato N, Hirata Y, Kyo S, Ono M, Nagai R. Age and preoperative total bilirubin level can stratify prognosis after extracorporeal pulsatile left ventricular assist device implantation. Circ J. 2011;75(1):121–8.
8. Takano H, Taenaka Y, Noda H, Kinoshita M, Yagura A, Tatsumi E, Sekii H, Umezu M, Nakatani T. Multi-institutional studies of the national cardiovascular center ventricular assist system: use in 92 patients. ASAIO Trans. 1989;35:541–4.
9. Takano H, Nakatani T, Taenaka Y. Clinical experience with ventricular assist systems in Japan. Ann Thorac Surg. 1993;55:250–5.
10. Saito S, Matsumiya G, Sakaguchi T, Fujita T, Kuratani T, Ichikawa H, Sawa Y. Fifteen-year experience with Toyobo paracorporeal left ventricular assist system. J Artif Organs. 2009;12:27–34.
11. Takatani S, Matsuda H, Hanatani A, Nojiri C, Yamazaki K, Motomura T, Ohuchi K, Sakamoto T, Yamane T. Mechanical circulatory support devices (MCSD) in Japan: current status and future directions. J Artif Organs. 2005;8:13–27.
12. Japanese Association for Clinical Ventricular Assist Systems. Japanese Registry for ventricular assist device. 2013. http://www.jacvas.com/VAS_registry2012.pdf. Accessed 28 May 2014. (in Japanese).
13. Nishinaka T, Taenaka Y, Tatsumi E, Ohnishi H, Homma A, Shioya K, Mizuno T, Tsukiya T, Mushika S, Hashiguchi Y, Suzuki A, Kitamura S. Development of a compact portable driver for a pneumatic ventricular assist device. J Airtif Organs. 2007;10:236–9.
14. Homma A, Taenaka Y, Tatsumi E, Akagawa E, Lee H, Nishinaka T, Takewa Y, Mizuno T, Tsukiya T, Kakuta Y, Katagiri N, Shimosaki I, Hamada S, Mukaibayashi H, Iwaoka W. Development of a compact wearable pneumatic drive unit for a ventricular assist device. J Artif Organs. 2008;11:182–90.
15. Gawlikowski M, Darłak M, Pustelny T, Kustosz R. Preliminary investigations regarding the possibility of acoustic resonant application for blood volume measurement in pneumatic ventricular assist device. Mol Quantum Acoust. 2006;27:89–96.
16. Gawlikowski M, Pustelny T, Kustosz R, Darłak M. Non invasive blood volume measurement in pneumatic ventricular assist device POLVAD. Mol Quantum Acoust. 2006;27:97–106.
17. Kamimura T, Homma A, Tsukiya T, Kakuta Y, Lee H, Tatsumi E, Taenaka Y, Kitamura S. Monitoring of diaphragm position in pulsatile pneumatic ventricular assisted device by ultrasound sensor (a new method for flow measurement in VAD). JSME Int J Ser C. 2004;47:1124–7.
18. Sasaki E, Nakatani T, Taenaka Y, Takano H, Hirose H. Novel method to determine instantaneous blood volume in pulsatile blood pump using electrical impedance. Artif Organs. 1994;18:603–10.

J Artif Organs
DOI 10.1007/s10047-014-0810-0

ORIGINAL ARTICLE

Artificial Lung / ECMO

Impact of bypass flow rate and catheter position in veno-venous extracorporeal membrane oxygenation on gas exchange in vivo

Konomi Togo · Yoshiaki Takewa · Nobumasa Katagiri · Yutaka Fujii · Satoru Kishimoto · Kazuma Date · Yuji Miyamoto · Eisuke Tatsumi

Received: 27 August 2014 / Accepted: 27 November 2014

Abstract The clinical use of veno-venous extracorporeal membrane oxygenation (VVECMO) in adult patients with respiratory failure is rapidly increasing. However, recirculation of blood oxygenated by ECMO back into the circuit may occur in VVECMO, resulting in insufficient oxygenation. The cannula position and bypass flow rate are two major factors influencing recirculation, but the relationship and ideal configuration of these factors are not fully understood. In the present study, we attempted to clarify these parameters for effective gas exchange. VVECMO was performed in eight adult goats under general anesthesia. The position of the drainage cannula was fixed in the inferior vena cava (IVC), but the return cannula position was varied between the IVC, right atrium (RA), and superior vena cava (SVC). At each position, the recirculation rates calculated, and the adequacy of oxygen delivery by ECMO in supplying systemic oxygen demand was assessed by measuring the arterial oxygen saturation (SaO_2) and pressure (PaO_2). Although the recirculation rates increased as the bypass flow rates increased, SaO_2 and PaO_2 also increased in any position of return cannula. The recirculation rates and PaO_2 were 27 ± 2 % and 162 ± 16 mmHg, 36 ± 6 % and 139 ± 11 mmHg, and 63 ± 6 % and 77 ± 9 mmHg in the SVC, RA and IVC position at 4 L/min respectively. In conclusion, the best return cannula position was the SVC, and a high bypass flow rate was advantageous for effective oxygenation. Both the bypass flow rates and cannula position must be considered to achieve effective oxygenation.

Keywords Veno-venous extracorporeal membrane oxygenation · Respiratory support · Cannulation · Bypass flow · Recirculation

K. Togo (✉) · Y. Takewa (✉) · N. Katagiri · Y. Fujii · S. Kishimoto · K. Date · E. Tatsumi
Department of Artificial Organs, National Cerebral and Cardiovascular Center Research Institute, 5-7-1 Fujishiro-dai, Suita, Osaka 565-8565, Japan
e-mail: togo.konomi.ri@ncvc.go.jp

Y. Takewa
e-mail: takewa@ncvc.go.jp

K. Togo · Y. Miyamoto
Department of Cardiovascular Surgery, Hyogo College of Medicine, 1-1 Mukogawa-cho, Nishinomiya-shi, Hyogo 663-8501, Japan

Introduction

Extracorporeal membrane oxygenation (ECMO) is used for patients with severe pulmonary or cardiorespiratory failure. There are two basic types of ECMO veno-arterial ECMO (VAECMO) and veno-venous ECMO (VVECMO). VAECMO is particularly favored for severe cardiac or cardiorespiratory failure, while VVECMO is used for patients with severe respiratory failure who do not improve on mechanical support or do not respond to medical treatment [1].

Although VVECMO is widely utilized in neonatal and pediatric patients with severe respiratory failure [2], its usage is controversial in adults owing to their low survival rates [3]. In 2000, Bartlett et al. reported that the survival rate of discharged patients with progressive respiratory failure was 88 % in 586 neonates, 70 % in 132 children, and 56 % in 146 adults [4]. The number of adult ECMO patients with respiratory failure increased considerably in 2009 with the H1N1 influenza pandemic and the publication of the Conventional Ventilation or ECMO for Severe Adult Respiratory failure (CESAR) trial results. Since

Published online: 05 December 2014

2011, approximately 400 cases yearly have been reported by the Extracorporeal Life Support Organization (ELSO) [5].

There are fewer complications associated with VVECMO than with VAECMO, which include systemic thromboembolism, limb ischemia, maldistribution of oxygen, and increased left ventricular wall tension [6]. Additionally, VVECMO offers the advantage of simple cannulation without requiring arterial puncture and, therefore, is easily implemented. However, because both the drainage and return cannulae are in a single vein in VVECMO, a variable proportion of oxygenated blood from the return cannula enters the drainage cannula, a condition known as recirculation. Recirculation during VVECMO may cause insufficient oxygenation. The four factors that can affect the magnitude of recirculation are cannula position, bypass flow rate, cardiac output (CO), and intravascular volume [7]. To date, the relationship between recirculation and effective oxygenation in VVECMO has not been thoroughly investigated in adults. In the present study, we attempted to clarify the effect of these variables on effective gas exchange.

Materials and methods

Animals

Eight adult goats with a mean body weight of 58.6 ± 0.6 kg were evaluated. They were maintained at the National Cerebral and Cardiovascular Center in accordance with the guidelines of the committee on animal studies. This study was approved by the Animal Investigation Committee of this institution.

Animal preparation

Anesthesia was induced with 10 mg/kg of ketamine administered intramuscularly (Daiichi-Sankyo Pharmaceutical Products Ltd., Tokyo, Japan). The goats were then tracheotomized and ventilated to maintain normal blood gas values. During the preparation for VVECMO, the goats were ventilated at a FiO_2 of 0.4–1.0, respiratory rate of 10–20 breaths/min, and a tidal volume of 10 mL/kg; anesthesia was maintained with isoflurane (2 ± 0.5 vol/100 mL in oxygen). A 14-G catheter (Argyle, Covidien, Tokyo, Japan) was inserted into the left external jugular vein for drug infusion. A 7.5-Fr Swan-Ganz Oximetry catheter (CCOmbo Volumetrics Pulmonary Artery Catheter, model 741HF75, Edwards, Irvine, CA, USA) was inserted into the left external jugular vein with the tip positioned in the pulmonary artery (PA) and a second 14-G catheter was inserted into the carotid artery to obtain blood samples. CO was measured using a Vigileo Monitor (Edwards, Irvine, CA, USA) and a FloTrac sensor (Edwards, Irvine, CA, USA). The utility of the Vigileo Monitor has been reported previously [8–10]. Because the FloTrac sensor can predict the CO based on the standard deviation of the arterial blood pressure, it only needed to be connected to the existing arterial blood pressure line. The thermodilution method cannot be used directly for CO measurements during ECMO; therefore, a combination of the Vigileo monitor and the FloTrac sensor were utilized. Because Hb and CO influence oxygen consumption and delivery, these conditions were maintained at a constant level for the maximum time possible.

The rectal temperature was monitored using a thermistor thermometer (Type T, copper-constantan thermocouple) and maintained at 36.5 ± 1.0 °C using a warm water mattress and heat exchanger. The vital and bypass flow data were recorded using Labchart 5 (ADInstruments Pty Ltd., Bella Vista, Australia).

ECMO circuit

An ECMO system (Endumo® 6000, Heiwa Bussan, Tokyo, Japan) comprising a ROTAFLOW® centrifugal pump (Maquet, Rastatt, Germany), a heparin-coated circuit (T-NCVC® coating; National Cerebral and Cardiovascular Center, Osaka, Japan and Toyobo, Osaka, Japan), and an oxygenator (BIOCUBE 6000®, Nipro, Osaka, Japan) was used [1, 11, 12]. The system was primed with Lactated Ringer's solution.

The goats were administered 300 units/kg of heparin, and the 20-Fr return and drainage cannulae (PCKC-V-20, Toyobo Co., Ltd., Osaka, Japan) were inserted into the right external jugular vein and the inferior vena cava (IVC) using the surgical cutdown method.

Experimental protocol

First, recirculation was visualized by angiography by administering contrast media into the ECMO outflow. Second, to create baseline conditions before starting ECMO, the ventilator setting was adjusted appropriately. And the mixed venous oxygen saturation was maintained at 40 ± 5 % as the baseline condition. The blood sample at baseline was taken after the stable baseline condition was maintained at least 5 min. To investigate blood oxygenation using ECMO alone under the conditions of eliminated native respiration, the ventilator was discontinued, and ECMO was initiated. The oxygenator was ventilated with 100 % O_2, and the V/Q ratio ($V = O_2$ gas flow rate, Q = bypass flow rate) was set at 1.0. During VVECMO, anesthesia was maintained with intravenous propofol at 0.5 mL/kg/h (Mylan Pharmaceutical Products Ltd., Osaka,

Japan). Third, to quantify the angiographic results, the recirculation rates were calculated under each condition by measuring the oxygen saturation as follows [13]:

$$\text{Recirculation rate} = \frac{\text{Oxygen saturation of the preoxygenator blood} - \text{Mixed venous oxygen saturation}}{\text{Oxygen saturation of the postoxygenator blood} - \text{Mixed venous oxygen saturation}}$$

This method is the gold standard of recirculation rate measurement in experimental settings [13]. Blood gas was measured with an automatic blood gas analyzer (Radiometer, ABL800 Flex Analyzer, Copenhagen, Denmark). Subsequently, the arterial oxygen saturation (SaO_2) and pressure (PaO_2) were measured under conditions of eliminated native respiration for 20 min. This experiment procedure was repeated in every cannula position and bypass flow rate, as shown below.

Position of the return and drainage cannulae, and bypass flow

The position of the return cannula was varied between the IVC, right atrium (RA), and superior vena cava (SVC), and the drainage cannula was fixed in the IVC (Fig. 1). Cannula positions were confirmed radiographically. The bypass flow rate was set from 1 to 4 L/min at each position. These data collection was taken 30–40 min after each change. Then, in consideration of existence of hysteresis, the order of the data collection in cannula positions and bypass flow rates was changed in every experiment.

Statistical analysis

All data are shown as mean ± standard error. Serial changes in recirculation rates, SaO_2, PaO_2, $PaCO_2$, Hb, and CO were analyzed by one-way analysis of variance (ANOVA). Bonferroni/Dunn's post hoc test was performed when a significant difference was detected in the one-way ANOVA. P values <0.05 were considered statistically significant. All data were analyzed using Statcel2 (the add-in forms on Excel).

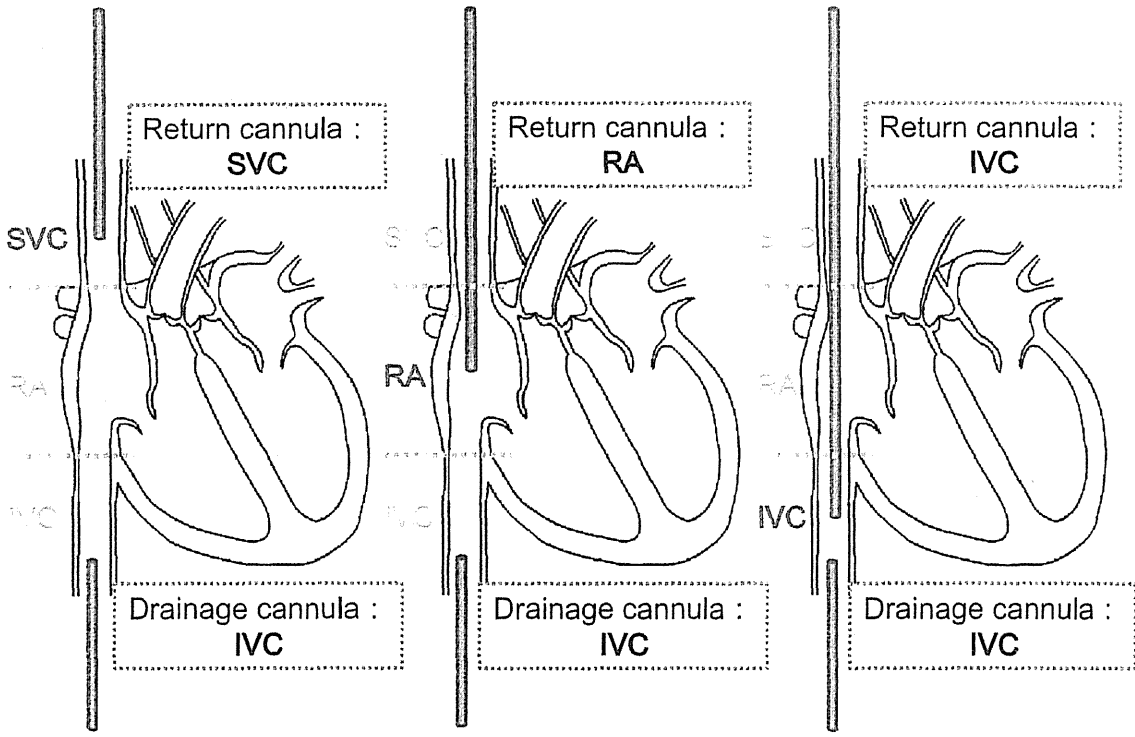

Fig. 1 Position of return and drainage cannulae. Schematic of heart and position of return and drainage cannulae. The *orange cannula* represents the return cannula; the *blue cannula* represents the drainage cannula. *IVC* inferior vena cava, *RA* right atrium, *SVC* superior vena cava

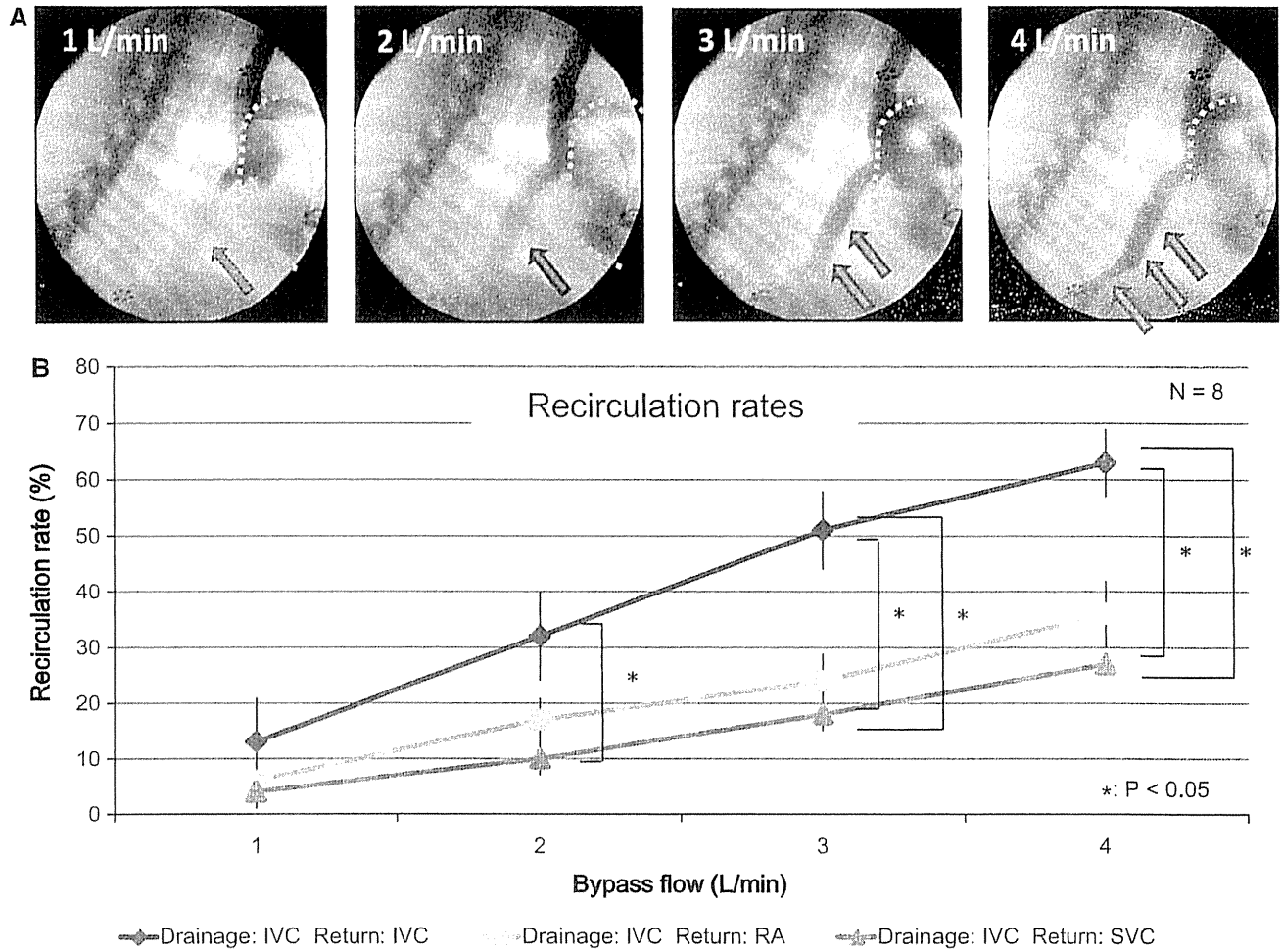

Fig. 2 Recirculation (angiography and recirculation rates). **a** Angiography on each bypass flow in the SVC return cannula position. The *red oval* represents the tip of return cannula in the SVC; the *blue oval* represents the tip of drainage cannula in the IVC; the *green section* represents the heart; the *orange arrow* indicates where recirculation occurs. The blood in the area indicated by the *orange arrow* flows from the return cannula to the drainage cannula. The contrast medium appears darker as the bypass flow rate increases. **b** The recirculation rates on each bypass flow. The return cannula positions are indicated by: *diamond markers* for IVC, *square markers* for RA, and *triangular markers* for SVC. The recirculation rates in the SVC and RA return cannula positions at 3 and 4 L/min were significantly lower than those in the IVC return cannula position ($P < 0.05$). *IVC* inferior vena cava, *RA* right atrium, *SVC* superior vena cava

Results

Recirculation

A representative angiogram showing the return cannula positioned in the SVC is shown in Fig. 2a. With the return cannula in this position, it is easy to understand the phenomenon of recirculation variation. Most of the blood exiting the return cannula flowed toward the PA. However, a small volume of blood entered the drainage cannula (Fig. 2a, arrows). The contrast medium gradually darkened as the bypass flow rate increased, and the increased recirculation was visually confirmed as the bypass flow rate increased.

Figure 2b summarizes the recirculation rates. At each return position, the recirculation rates increased as the bypass flow rates increased. The recirculation rate in the IVC return cannula group was higher than those in the SVC and RA groups. When the bypass flow rates were 3 and 4 L/min, the recirculation rate in the IVC position was significantly higher than the recirculation rates in the SVC and RA positions ($P < 0.05$).

Blood oxygenation

Figures 3 and 4 illustrate the SaO_2 and the PaO_2 values according to the cannula positions at bypass flow rates from 1 to 4 L/min. The SaO_2 and PaO_2 increased as the bypass flow rates increased. When the bypass flow rates were higher than 2 L/min in the SVC and RA positions, the SaO_2 was maintained at greater than 80 %. When the bypass flow rate was 4 L/min in the SVC and RA positions,

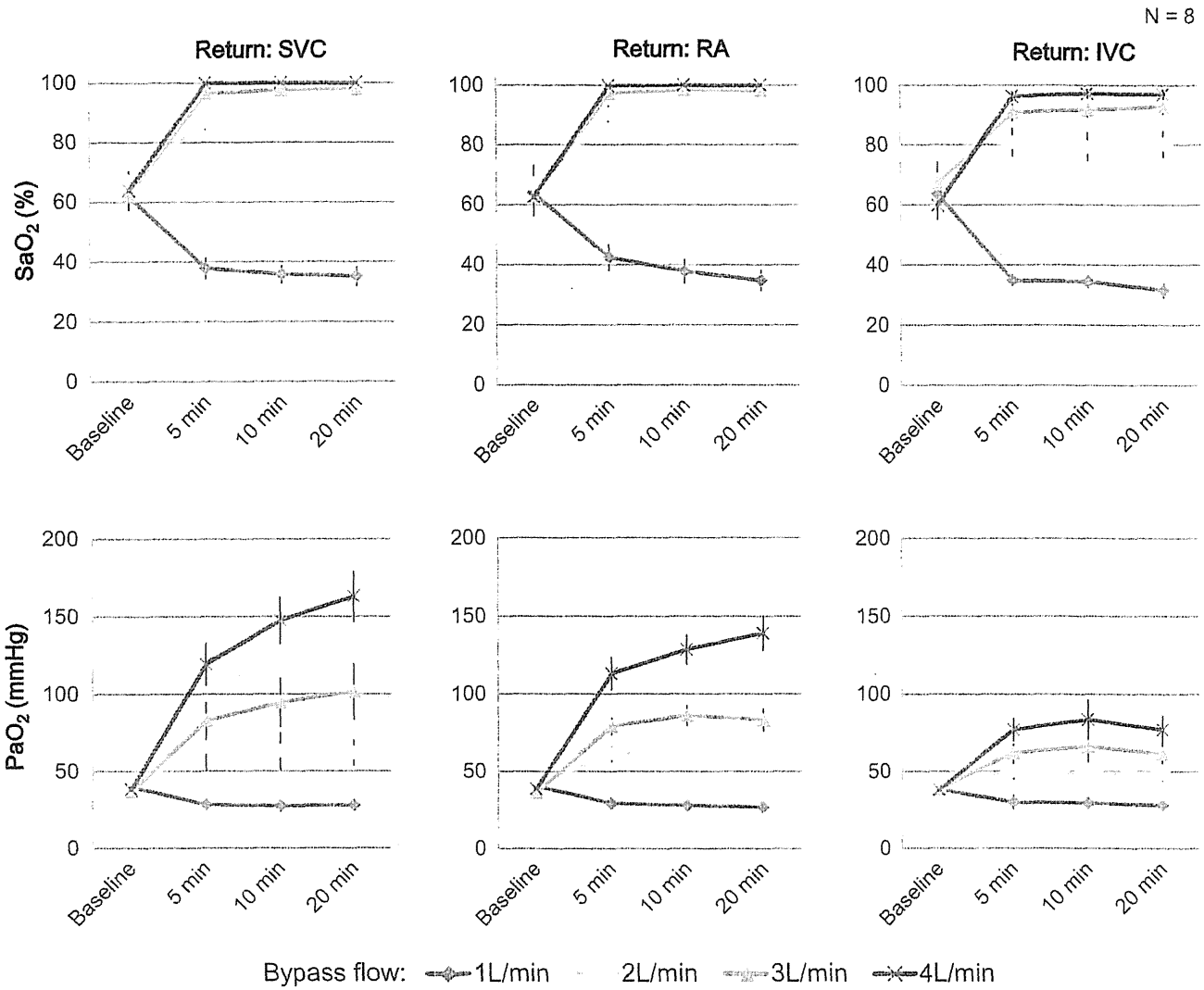

Fig. 3 Variation of oxygenation: arterial oxygen saturation (SaO_2) and pressure (PaO_2). The variation of the SaO_2 and the PaO_2 before VVECMO (in baseline condition) and during VVECMO for 20 min ($n = 8$). The SaO_2 showed no significant difference in any position at each bypass flow. The PaO_2 was significantly higher in the SVC position at 3 and 4 L/min than that in the IVC position ($P = 0.02$ and $P < 0.01$). *IVC* inferior vena cava, *RA* right atrium, *SVC* superior vena cava

the SaO_2 was 100 %. Interestingly, at 20 min, the PaO_2 was higher in the SVC position than in the RA position (162.9 ± 16.6 vs 139.0 ± 11.5 mmHg), although the difference was not statistically significant ($P = 0.15$). The PaO_2 in the SVC return cannula position 20 min after initiating ECMO support was significantly higher than that in the IVC return cannula position (162.9 ± 16.6 vs 77.0 ± 9.2 mmHg, respectively, $P < 0.01$). The SaO_2 and PaO_2 values in the IVC return cannula group were lower than those at the other two return cannula positions.

Blood carbon dioxide removal ($PaCO_2$ and pH)

Figure 4 shows the partial pressure of carbon dioxide in the arterial blood ($PaCO_2$) and the blood pH. The mean pH, $PaCO_2$, HCO_3, and BE before VVECMO were 7.24 ± 0.01, 58.3 ± 0.9, 23.6 ± 0.3, and −3.4 ± 0.2, respectively, and respiratory acidosis was induced in all the goats. After initiating VVECMO, the $PaCO_2$ decreased as the bypass flow rates increased, except at 1 L/min. When the bypass flow rate was maintained at 1 L/min, the $PaCO_2$ tended to increase over a 20-min period after initiating VVECMO. The $PaCO_2$ approached the normal level of 45 mmHg at a bypass flow rate of 2 L/min in the SVC or RA return cannula position and at a bypass flow of 3 L/min in all return cannula positions. The $PaCO_2$ and pH showed no significant differences between the return cannula positions at each bypass flow. When the bypass flow rate was maintained at greater than 3 L/min for 20 min, the pH approached the normal range. The mean HCO_3 during

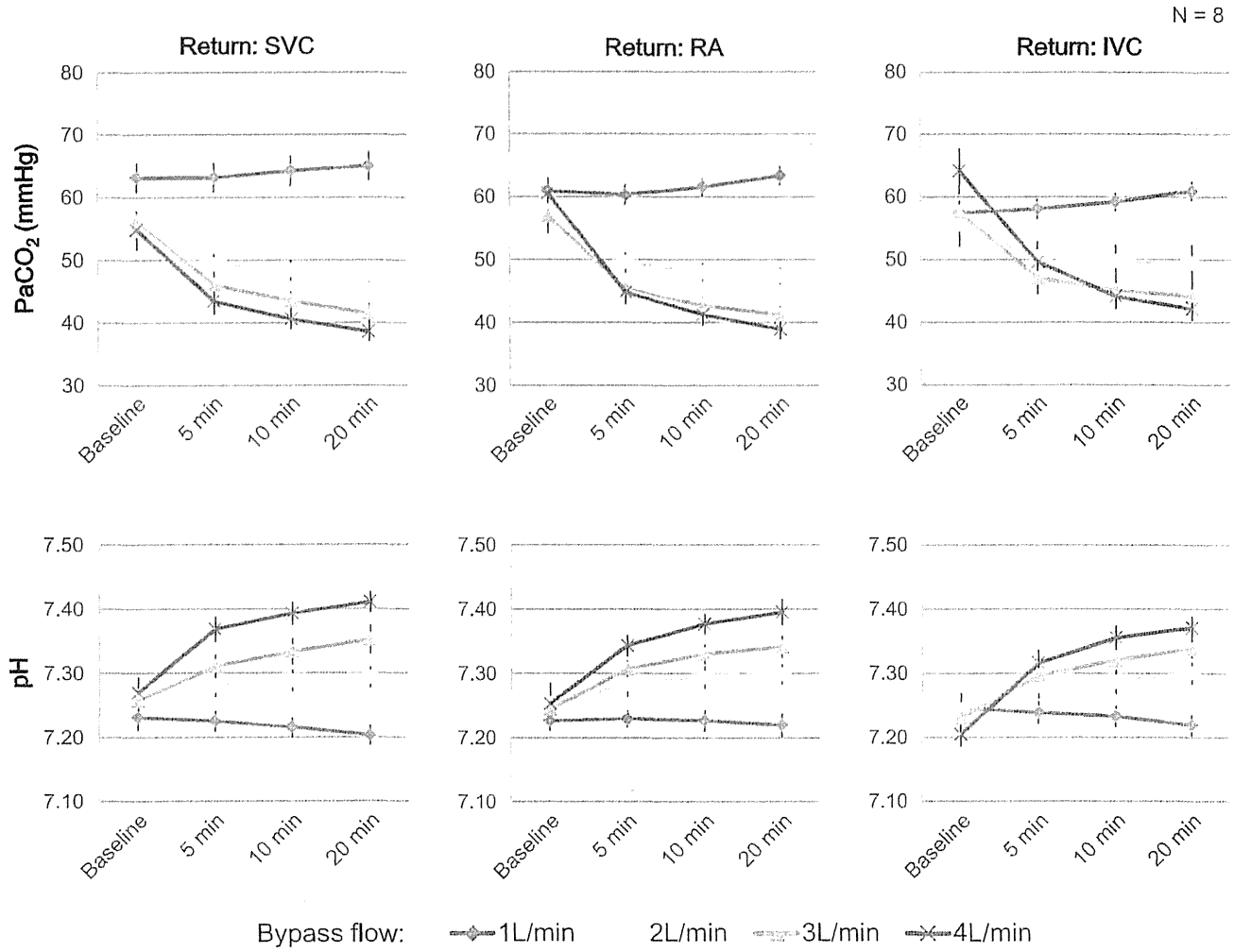

Fig. 4 Variation of carbon dioxide removal: Partial pressure of carbon dioxide in arterial blood ($PaCO_2$) and pH. The $PaCO_2$ and pH before VVECMO (in baseline condition) and during VVECMO ($n = 8$). $PaCO_2$ and pH showed no significant difference in any position at each bypass flow. *IVC* inferior vena cava, *RA* right atrium, *SVC* superior vena cava

VVECMO was 22.5 ± 0.2 and were close to the normal range.

Measurement conditions

The mean hemoglobin (Hb) was 9.8 ± 0.1 mg/dL, and the mean CO was 4.9 ± 0.1 L/min. These values showed no significant differences among the positions at each bypass flow rate.

Discussion

This study determined the recirculation and blood oxygenation rates in VVECMO under several conditions. We demonstrated that it is preferable to position the return cannula in the SVC, and a high bypass flow is better for effective oxygenation than a low bypass flow.

VVECMO can cause recirculation, which results in inadequate oxygenation and should be minimized. Heard et al. also reported that the cannula position, bypass flow rate, CO, and intravascular volume influence recirculation [7]. Of these four factors, CO and intravascular volume are passive factors that vary primarily due to the patient's condition. In the present study, we focused on the cannula position and bypass flow rate because these are measurable active factors.

VVECMO is inserted using two techniques: dual cannulation with return and drainage cannulae, and single cannulation comprising one cannula with a double-lumen catheter (DLC) that allows both return and drainage [1, 14]. The use of single cannulation has increased in several countries, though it has not yet been approved by Japanese regulatory authorities. The combined return and drainage cannulae sites are often used: the femoral vein (FV) drainage/internal jugular vein (IJV) return, IJV drainage/

FV return, and FV drainage/FV return in dual cannulation. Rich et al. compared the methods of drainage from the FV with RA return to drainage from the RA with FV return and found that the former configuration provides superior oxygenation [15]. Based on these and other results, the most frequent method is to insert the drainage cannula at the FV with its tip placed in the IVC, which allows a sufficient bypass flow rate, and insert the return cannula insertion at the IJV with its tip placed in the SVC, RA, or IVC. Therefore, in the present study, we placed the return cannula in the SVC, RA, and IVC. As for bypass flow rates, according to the ELSO guidelines, a blood flow rate between 60 and 80 mL/kg/min is required to fully support an adult [16]. We used adult goats weighing approximately 60 kg, and the maximum bypass flow rate was set at 4 L/min and data were collected from 1 to 4 L/min.

The recirculation rate was calculated by the gold standard method in this study [13]. Mixed venous blood from the PA is necessary when applying the formula of this method. The mixed venous blood is present in the PA, and it does not include oxygenated blood which flows from ECMO. However, ECMO-oxygenated and unoxygenated venous blood are mixed in the PA after starting VVECMO. Therefore, we used the blood in the PA before starting ECMO with mixed venous blood. Our results demonstrated that the recirculation rate was the lowest when the return cannula was positioned in the SVC. Dual cannulation allows the distance between the return and drainage cannulae to be varied. Conversely, for single cannulation, the distance between the return and drainage ports is fixed. The Avalon Elite® DLC (Avalon Laboratory, Los Angeles, CA, USA), which is available for use in several countries, has drainage ports in the SVC and IVC and the return port in the RA [1, 17, 18]. To date, nearly all studies on recirculation rates for adults performed single cannulation using the Avalon Elite® DLC. Wang et al. reported that the recirculation rate using the Avalon Elite® DLC was 3.3 ± 0.2 % when the bypass flow rate was 2 L/min, whereas Körver et al. reported a rate of 2 % at a bypass flow rate of 4.3 L/min [14, 17]. The recirculation rates in those studies were lower than those in all the return positions used in our experiment. When the distance between the drainage and return ports was large, the recirculation rate was generally high in both single and dual cannulations. For the Avalon Elite® DLC, the distance between the drainage port and the return port was 9.4 cm [14]. In our experiment, the mean distance from the tip port of the drainage cannula in the IVC to the tip port of the return cannula in the RA was 10 cm. The distance between the return and drainage ports when the return cannula was placed in the RA was nearly identical to the distance in the aforementioned studies. The difference between single cannulation and dual cannulation is in the flow direction of the returning blood. The Avalon Elite® DLC is designed to allow the return port of the RA to face the tricuspid valve [14]. However, in our experiment, the blood exiting the return cannula flows linearly toward the drainage cannula placed in the IVC, which easily causes recirculation because the return cannula and drainage cannula ports face each other. We surmise that this is the reason for the higher recirculation rate in our experiment than that in other reports. Additionally, we investigated whether oxygen delivery by the VVECMO under each condition adequately accommodated the demands of the systemic organs by measuring the arterial oxygen saturation (SaO_2) and pressure (PaO_2) under conditions of eliminated native respiration. Our results demonstrated that the PaO_2 was highest in the SVC return position. From the point of view of recirculation and blood oxygenation, it is preferable to place the return cannula in the SVC.

In the international ECLS association ELSO guidelines, a SaO_2 of greater than 80 % are defined as benchmarks of adequate oxygenation in VVECMO [16]. In this study, a bypass flow rate of 2 L/min in the SVC or RA return positions, or 3 L/min in the IVC return positions was required because the SaO_2 was at least 80 %. Wang et al. reported that a 2 L/min bypass flow rate was required for adequate gas exchange in nearly all patients, which is similar to our results [14]. Schmidt et al. reported that the oxygen saturation increases as the ratio of CO to bypass flow rate decreases [19]. Oxygen saturation must be monitored constantly using a pulse oximeter or an oxygen saturation measuring instrument incorporated in the ECMO circuit.

When the bypass flow rate was higher than 2 L/min in the SVC or RA return cannula position, or 3 L/min in the IVC return cannula position, the $PaCO_2$ approached the normal range. The $PaCO_2$ decreased as bypass flow rates increased, except at a flow rate of 1 L/min. The factors affecting carbon dioxide removal are the sweep gas flow rate and oxygenator surface area [19, 20]. Then, we investigated whether $PaCO_2$ varies with the V/Q while maintaining the bypass flow at 1 L/min. When V/Q was increased from 1 to 3 and 5, the $PaCO_2$ decreased from 61.9 and 60.1 to 51.7 and 47.2 mmHg, respectively, after 20 min ($n = 1$) in the SVC return position. We will investigate carbon dioxide removal in future experiments.

The data collection was taken at least 30–40 min at one cannula position and one bypass flow rate. Because data collection at each condition was time consuming, it was only performed for 20 min in each goat. The PaO_2 may increase and $PaCO_2$ may decrease if VVECMO was continued for more than 20 min. Moreover, the mixed venous oxygen saturation was set in 40 ± 5 % as the baseline condition in this study, and this value might affect changes of SaO_2, PaO_2, and $PaCO_2$.

Conclusions

We demonstrated that it is preferable to position the return cannula in the SVC. Additionally, the SaO_2 and PaO_2 increased as the bypass flow rates increased from 1 to 4 L/min, despite the increased recirculation rates. Therefore, a high bypass flow is beneficial for effective oxygenation. Both the bypass flow rates and cannula position must be considered to achieve effective oxygenation depending on the condition of each patient. Last, DLCs are currently used in countries other than Japan with little recirculation in adults. We expect that DLCs for VVECMO will also become available in Japan.

Conflict of interest The authors declare no conflict of interest.

References

1. Ota K. Advances in artificial lungs. J Artif Organs. 2010;13:13–6.
2. Herlihy JP, Loyalka P, Jayaraman G, Kar B, Gregoric ID. Extracorporeal membrane oxygenation using the TandemHeart System's catheters. Tex Heart Inst J. 2009;36:337–41.
3. Schuerer DJ, Kolovos NS, Boyd KV, Coopersmith CM. Extracorporeal membrane oxygenation: current clinical practice, coding, and reimbursement. Chest. 2008;134:179–84.
4. Bartlett RH, Roloff DW, Custer JR, Younger JG, Hirschl RB. Extracorporeal life support: the University of Michigan experience. JAMA. 2000;283:904–8.
5. Paden ML, Conrad SA, Rycus PT, Thiagarajan RR. Extracorporeal life support organization registry report 2012. ASAIO J. 2013;59:202–10.
6. MacLaren G, Combes A, Bartlett RH. Contemporary extracorporeal membrane oxygenation for adult respiratory failure: life support in the new era. Intensive Care Med. 2012;38:210–20.
7. Heard ML, Davis J, Fortenberry JD. Principles and practice of venovenous and venoarterial extracorporeal membrane oxygenation. In: Short BL, Williams L, editors. ECMO specialist training manual. 3rd ed. Ann Arbor: ELSO; 2010. p. 59–76.
8. Pratt B, Roteliuk L, Hatib F, Frazier J, Wallen RD. Calculating arterial pressure-based cardiac output using a novel measurement and analysis method. Biomed Instrum Technol. 2007;41:403–11.
9. Langewouters GJ, Wesseling KH, Goedhard WJ. The static elastic properties of 45 human thoracic and 20 abdominal aortas in vitro and the parameters of a new model. J Biomech. 1984;17:425–35.
10. Bridges EJ. Arterial pressure-based stroke volume and functional hemodynamic monitoring. J Cardiovasc Nurs. 2008;23:105–12.
11. Nishinaka T, Tatsumi E, Katagiri N, Ohnishi H, Mizuno T, Shioya K, Tsukiya T, Homma A, Kashiwabara S, Tanaka H, Sato M, Taenaka Y. Up to 151 days of continuous animal perfusion with trivial heparin infusion by the application of a long-term durable antithrombogenic coating to a combination of a seal-less centrifugal pump and a diffusion membrane oxygenator. J Artif Organs. 2007;10:240–4.
12. Kusajima K, Hoashi T, Kagisaki K, Yoshida K, Nishigaki T, Hayashi T, Ichikawa H. Clinical experience of more than 2 months usage of extracorporeal membrane oxygenation (Endumo®4000) without circuit exchange. J Artif Organs. 2014;17:99–102.
13. Van Heijst AF, van der Staak FH, de Haan AF, Liem KD, Festen C, Geven WB, van de Bor M. Recirculation in double lumen catheter veno-venous extracorporeal membrane oxygenation measured by an ultrasound dilution technique. ASAIO J. 2001;47:372–6.
14. Wang D, Zhou X, Liu X, Sidor B, Lynch J, Zwischenberger JB. Wang-Zwische double lumen cannula-toward a percutaneous and ambulatory paracorporeal artificial lung. ASAIO J. 2008;54:606–11.
15. Rich PB, Awad SS, Crotti S, Hirschl RB, Bartlett RH, Schreiner RJ. A prospective comparison of atrio-femoral and femoro-atrial flow in adult venovenous extracorporeal life support. J Thorac Cardiovasc Surg. 1998;116:628–32.
16. Extracorporeal Life Support Organization (ELSO) General Guidelines for all ECLS Cases (Version 1.3). Extracorporeal Life Support Organization. http://www.elso.org/resources/guidelines?download=17:elso-guidelines-generalv11 (2013). Accessed 8 Aug 2014.
17. Körver EP, Ganushchak YM, Simons AP, Donker DW, Maessen JG, Weerwind PW. Quantification of recirculation as an adjuvant to transthoracic echocardiography for optimization of dual-lumen extracorporeal life support. Intensive Care Med. 2012;38:906–9.
18. Javidfar J, Brodie D, Wang D, Ibrahimiye AN, Yang J, Zwischenberger JB, Sonett J, Bacchetta M. Use of bicaval dual-lumen catheter for adult venovenous extracorporeal membrane oxygenation. Ann Thorac Surg. 2011;91:1763–9.
19. Schmidt M, Tachon G, Devilliers C, Muller G, Hekimian G, Bréchot N, Merceron S, Luyt CE, Trouillet JL, Chastre J, Leprince P, Combes A. Blood oxygenation and decarboxylation determinants during venovenous ECMO for respiratory failure in adults. Intensive Care Med. 2013;39:838–46.
20. Rees NJ, Waldvogel J. Extracorporeal life support (ECLS) physiology. In: Short BL, Williams L, editors. ECMO specialist training manual. 3rd ed. Ann Arbor: ELSO; 2010. p. 37–48.

European Journal of Cardio-Thoracic Surgery Advance Access published October 7, 2014

European Journal of Cardio-Thoracic Surgery (2014) 1-6
doi:10.1093/ejcts/ezu364

ORIGINAL ARTICLE

BASIC SCIENCE

Alternative approach for right ventricular failure after left ventricular assist device placement in animal model†

Tomohiro Saito[a], Koichi Toda[b,*], Yoshiaki Takewa[a], Tomonori Tsukiya[a], Toshihide Mizuno[a], Yoshiyuki Taenaka[a] and Eisuke Tatsumi[a]

[a] Department of Artificial Organs, National Cerebral and Cardiovascular Center Research Institute, Osaka, Japan
[b] Department of Cardiovascular Surgery, Osaka University Graduate School of Medicine, Osaka, Japan

* Corresponding author. 2-2, Yamada-Oka, Suita, Osaka 565-8565, Japan. Tel: +81-6-68793154; fax: +81-6-68793163; e-mail: ktoda2002@yahoo.co.jp (K. Toda).

Received 17 June 2014; received in revised form 8 August 2014; accepted 13 August 2014

Abstract

OBJECTIVES: Right ventricular failure after left ventricular assist device (LVAD) implantation is associated with high mortality. This study was designed to evaluate the effectiveness of an atrial septostomy with a membrane oxygenator incorporated in an LVAD as a novel approach for right ventricular failure after LVAD implantation.

METHODS: The outflow and inflow cannulae were placed in the carotid artery and left ventricular apex, respectively. A centrifugal pump and an oxygenator were sequentially placed between the inflow and outflow cannulae in seven anesthetized goats. While right ventricular failure was induced by pulmonary artery banding, a balloon atrial septostomy was performed using a 19-mm balloon catheter under echocardiographic guidance. We investigated the effects of the interatrial shunt on LVAD flow and haemodynamics.

RESULTS: Development of right ventricular failure decreased LVAD flow (2.7 ± 0.6–0.9 ± 0.6 l/min), causing a state of shock [mean arterial pressure (MAP) of 41 ± 12 mmHg]. Following a balloon atrial septostomy, LVAD flow and MAP were significantly improved to 2.7 ± 0.4 l/min ($P < 0.001$) and 53 ± 18 mmHg ($P = 0.006$), respectively, while right atrial pressure decreased from 18 ± 5 to 15 ± 5 mmHg ($P = 0.001$). Furthermore, arterial blood oxygenation was maintained by the membrane oxygenator incorporated in the LVAD.

CONCLUSIONS: In the present model of right ventricular failure after LVAD implantation, LVAD flow was significantly increased and haemodynamics improved without compromising systemic oxygenation by the use of an interatrial shunt and a membrane oxygenator incorporated in the LVAD. Our results indicate that this novel approach may be less invasive for a right ventricular failure after LVAD implantation.

Keywords: Circulatory assist device • Animal model • Heart failure • extracorporeal membrane oxygenation

INTRODUCTION

Right ventricular failure is a critical complication after implantation of a left ventricular assist device (LVAD) and causes a significant increase in mortality [1, 2]. Although the use of a right ventricular assist device (RVAD) declined after the introduction of the implantable continuous flow pump, along with the use of inhaled nitric oxide and phosphodiesterase inhibitors to lower pulmonary vascular resistance and restore right ventricular function in patients with LVAD [3, 4], 13% of patients still required an RVAD in addition to LVAD implantation [5]. Since additional implantation of an RVAD involves further surgical stress, the prognosis of LVAD patients who require an RVAD is poor [6]. Management of two different assist devices creates additional complications, including a two-fold increase in infections, a three-fold increase in neurological problems and a four-fold increase in bleeding complications [5]. In order to improve the outcome of the patients who required RVAD after LVAD implantation, less invasive right ventricular supports including a pulsatile catheter pump [7] and a percutaneous RVAD with CentriMag [8] were tested clinically. However, implantation of the pulsatile catheter pump required a thoracotomy and percutaneous RVAD required placement of a relatively long cannula from the internal jugular vein to the pulmonary artery and from the femoral vein to the right atrium, which may facilitate thrombus formation around cannulae [9].

Balloon atrial septostomy is a time-tested less invasive procedure that can be performed in a percutaneous manner and has been successfully utilized for congenital cardiac anomalies for mixing deoxygenated blood in the atrium [10]. This procedure has also been used for right ventricular failure in patients with primary pulmonary hypertension [11–13]. The concept aims at creating a 'safety valve' by unloading the right ventricle and increasing left ventricular preload and output. Its validity was demonstrated in a clinical setting [11–13] as well as an animal study [14]. However, this concept has never been applied in case of right ventricular failure after LVAD implantation. The aim of the present study was to elucidate the effectiveness of an atrial septostomy with a

† Presented at the 59th Annual Meeting of The Southern Thoracic Surgical Association, Naples, FL, USA, 7–10 November 2012.

membrane oxygenator incorporated in LVAD as a novel approach for right ventricular failure after LVAD implantation in an acute animal model.

MATERIALS AND METHODS

Surgical preparation

All animals received humane care in compliance with the 'Principles of Laboratory Animal Care' formulated by the National Society for Medical Research, and the 'Guide for the Care and Use of Laboratory Animals,' prepared by the National Academy of Science and published by the National Institute of Health (NIH Publication 86-23, revised 1985). In addition, all experiments were approved by the Animal Experiment Ethics Committee of the National Cerebral and Cardiovascular Center Research Institute and performed within the guidelines prepared with the guidance of veterinarians.

Seven adult goats with a mean weight of 59 ± 8 kg (range, 54-70 kg) were used. The animals were anaesthetized with an intramuscular injection of ketamine (Daiichi Sankyo Co. Ltd, Tokyo, Japan) (10 mg/kg) and inhaled isoflurane (Air Water, Inc., Osaka, Japan). After a tracheotomy, the animals were ventilated with breathing frequency set between 10 and 20/min and a maximum airway pressure not greater than 30 mmHg. In a right decubitus position, 1 mg/kg of suxamethonium (Astellas Pharma, Inc., Tokyo, Japan) was intravenously administered prior to the skin incision and general anaesthesia was maintained by inhaled isoflurane. Through a sixth left intercostal thoracotomy, the pericardium was opened and the heart exposed. Pressure monitoring lines were inserted into the left internal thoracic artery, pulmonary trunk and right and left atriums, and were connected to pressure transducers. An electric magnetic flow meter (EMF-1000; Nihon Kohden, Tokyo, Japan) was set at the pulmonary trunk for flow monitoring. In parallel with the thoracic manipulation, the left carotid artery was exposed and prepared for cannulation of the outflow cannula.

Following systemic heparinization (300 U/kg), an apical sewing ring was sutured with eight buttressed sutures. Inflow (Nipro inflow cannula 24 F; Nipro, Osaka, Japan) and outflow (Bio-Medicus Femoral cannula 21 F; Medtronic, Minneapolis, MN, USA) cannulae were placed in the left ventricular apex and left carotid artery, respectively, and connected to a centrifugal pump (Jostra RotaFlow; Maquet Cardiopulmonary AG, Hirrlingen, Germany), in which an extracorporeal membrane oxygenator (Biocube 6000; Nipro, Osaka, Japan) was incorporated between the centrifugal pump and outflow cannula, as shown in Fig. 1. LVAD flow was measured using an ultrasonic flow meter (TS420; Transonic Systems, Inc., Ithaca, NY, USA) placed on the outflow cannula. The rotational speed of the pump was increased to between 2200 and 3300 rpm until maximum effective flow was obtained, and then maintained at nearly constant speed during the experiment. An 80% fraction of inspiratory oxygen with a 1 : 1 gas-to-blood flow ratio was continuously delivered to the membrane oxygenator during the experiment.

After the LVAD was placed, the proximal pulmonary trunk was encircled by a 1-cm wide Teflon felt for pulmonary artery banding. By tightening the Teflon felt under flow monitoring, pulmonary artery flow was regulated at approximately 1-2 l/min. A marking stitch was made on the Teflon felt to provide a constant experimental condition mimicking right ventricular failure.

Subsequently, a purse-string suture with tourniquet was placed at the left atrial wall to control bleeding. Then, the atrial septum was identified by direct echocardiography (Vivid 7 Pro; GE Medical Systems, Inc., Raleigh, NC, USA). Under echocardiographic guidance, the atrial septum was punctured using an 8-F introducer via the left atrial wall. A 5-F Miller balloon atrial septostomy catheter (Edwards Lifesciences Japan, Tokyo, Japan) was advanced into the right atrium cavity through the introducer using the Seldinger technique. After the balloon was inflated to 19 mm in

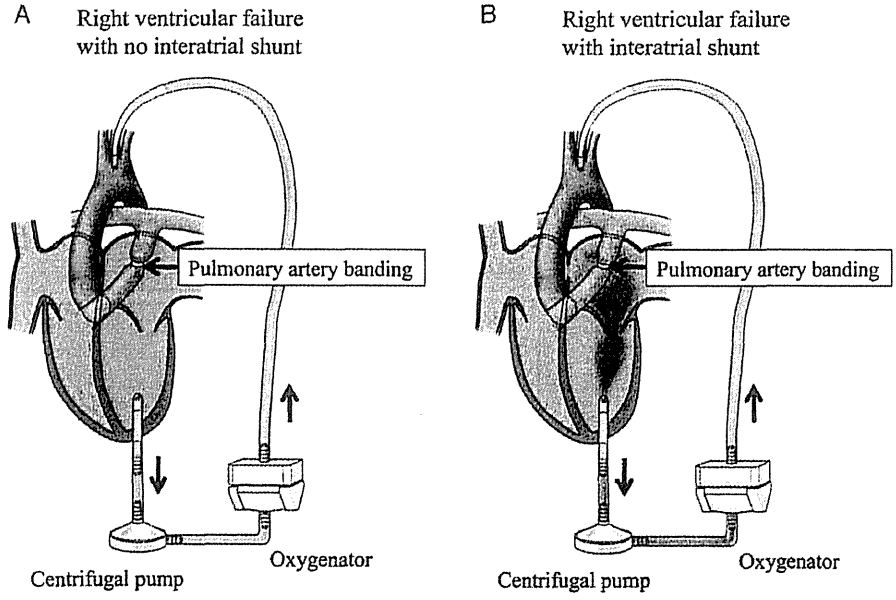

Figure 1: Schematic drawing of an experimental model. Inflow and outflow cannulae are placed in the left ventricular apex and left carotid artery, respectively and the centrifugal pump and membrane oxygenator are sequentially placed between the inflow and outflow cannulae. After left ventricular support is initiated, right ventricular failure is induced by pulmonary artery banding (**A**). After the interatrial shunt is opened, deoxygenated blood is drained from the right atrium to the left atrium and ventricle and oxygenated by a membrane oxygenator in the circuit (**B**).